Demonstrating a Multi-Depth Focused Laser Differential Interferometer Based on Chromatic Dispersion

Rachel U. Constantin* and Sophia C. Edwards†
The University of Tennessee-Knoxville, Knoxville, TN, 37995, USA
The University of Tennessee Space Institute, Tullahoma, TN, 37388, USA

Mark Gragston‡
The University of Tennessee-Knoxville, Knoxville, TN, 37995, USA
The University of Tennessee Space Institute, Tullahoma, TN, 37388, USA

This paper reviews a modified focused laser differential interferometer (FLDI) that uses two lasers to create focused points along the optical axis to potentially measure three-dimensional flow. The FLDI setup uses the wavelength dependence of the index of refraction to achieve the beam pairs focusing on different planes along the optical axis. This effect was modeled with simple ray tracing calculations for red and green laser light and compared to the actual setup using beam profiler images taken near the focal regions. A simple tube jet experiment shows that all the FLDI beam pairs act as expected, showing highly resolved turbulent spectra. Throughout the experiment, the FLDI instrument can still selectively reduce path integration effects, which are key for use in high-speed facilities. This modified FLDI system potentially allows for measurements of three-dimensional flow disturbances and convective velocities, which also allows for an additional measurement point for the correlation of turbulent fluctuations.

I. Nomenclature

$FLDI$	=	Focused Laser Differential Interferometry
f	=	Focal Length
n	=	Index of Refraction
R_1, R_2	=	Radii of Curvature for Lens Faces
n_D	=	Nominal Design Index of Refraction for a Lens
f_D	=	Nominal Design Focal Length for a Lens

II. Introduction

Focused laser differential interferometry (FLDI) is a laser diagnostic technique used to determine highly accurate density disturbances at the designated region in hypersonic flows [1, 2]. These density fluctuations can be correlated to quantitative velocity readings [3–5]. One example of how it is a valuable technique, FLDI can be used instead of embedding thermocouples and pressure transducers within the model. Since FLDI is setup outside of the model it can easily be moved to measure all points along the model in the flow unlike other measurement tools. FLDI can be traced back to the 1960s when the invention of lasers, a monochromatic light with stability, helped the precision of interferometry measurement tools. One example is a laser differential interferometry (LDI), it works by comparing the phase shift between two different beams, but the sensitivity region is the whole test section. To combat the large sensitivity region of an LDI, Smeets and George developed FLDI [6]. They used a lens to focus the beams down to a point and, therefore, minimized the sensitivity region of the system to a focused area. Jewell *et al.* [7] took the FLDI a step further by cross-correlating the two beams to prove the capability of velocity measurements from an FLDI system. Houpt *et al.* [8] and Hopkins *et al.* [9] closed a large research gap in the boundary layer transition experiments by changing the shape of the FLDI beam from a circular to a thin sheet using a cylindrical lens. Using a cylindrical lens

*Undergraduate Researcher, Department of Mechanical, Aerospace, and Biomedical Engineering, AIAA Student Member
†Undergraduate Researcher, Department of Mechanical, Aerospace, and Biomedical Engineering, AIAA Student Member
‡Assistant Professor, Department of Mechanical, Aerospace, and Biomedical Engineering, AIAA Member

improves the ability of the FLDI to take data near a flat wall or boundary layer transition data. To change the shape of the FLDI to fit any model of any experiment, Gragston *et al.* [10, 11] added defractors to the FLDI system. This allows for a variable number of beam pairs and orientations of said beam pairs. Through testing, it was determined that dichromic mirrors were negligible to the function of FLDI, so researchers were able to do Schlieren within the optical path of the FLDI. The addition of Schlieren allows for research to see the whole image of the density fluctuations in the focused and surrounding areas. Schlieren is non intrusive and can help explain certain anomalies in data. A focused laser differential interferometer (FLDI) is a highly versatile measurement tool for boundary layer transition, resolution of turbulent flows, acoustics, and etc. FLDI has low sensitivity outside of the focal region of the system and high sampling rates exceeding 1 MHz. FLDI is an ideal non intrusive tool for ground testing facilities and can collect data inside a high-speed tunnel through the outer walls, even next to the flat wall. Due to the Gladstone-Dale relation, the interference between each beam relates to the density fluctations of the surrounding fluid [12, 13]. The wavelength dependence of the index of refraction allows for two different focal points along the FLDI optical path. Using two lasers with different wavelengths, each beam path will be slightly different due to the index of refraction, causing the beams to focus on different locations along the optical path. Eventually, to further the research, an addition of a spatial light modulator (SLM) could also make it possible to shape the beam pairs in any arbitrary shape allowing to take measurements along the shape of models [14].

$$\frac{1}{f} = [n(\lambda) - 1]\left(\frac{1}{R_1} - \frac{1}{R_2}\right) = [n(\lambda) - 1]R \tag{1}$$

$$f(\lambda) = f_D \frac{n_D - 1}{n(\lambda) - 1} \tag{2}$$

This paper analyzes a recent advancement of the FLDI, using a second laser to exploit the wavelength dependence of the index of refraction. Therefore, the FLDI system can focus on two planes, leading to three-dimensional flow measurements.

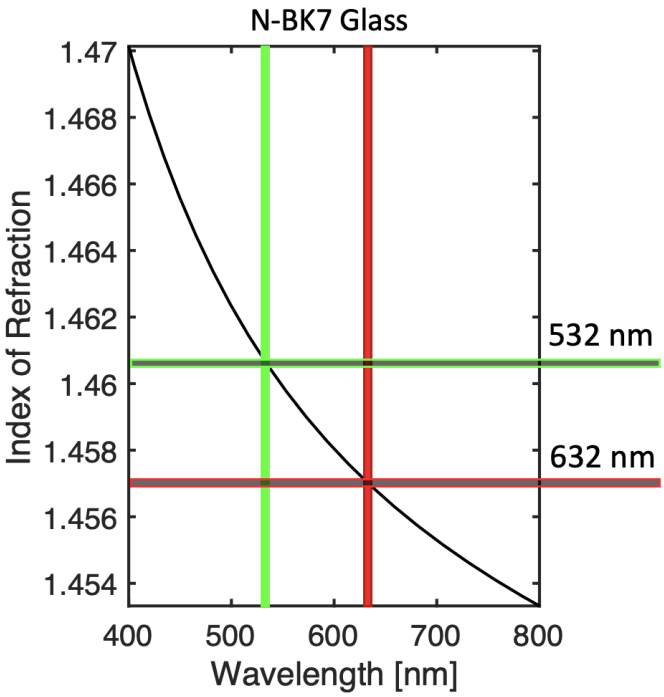

Fig. 1 This graph represents the index of refraction of N-BK7 Glass for each wavelength used in this experiment [15]. The wavelengths are color coded and labeled on each line.

The index of refraction, a property that demonstrates how light is either bent or slowed down through a medium compared to a vacuum. In N-BK7 Glass, the index of refraction varies from the wavelength due to dispersion when the speed of light is dependent on the wavelength or frequency. Equation 1 is the focal length of a light beam through a lens, assuming the thin lens analysis [16]. Where λ is the wavelength, n is the index of refraction, and R is the lens's curvature radius used in the experiment. Since both of the lasers move through the same lens on the same optical path, the lens's curvature radius can be thought of as one, labeled R, on the right side of equation 1. Through optical matrix and Eq. 2, the focal length of each individual laser can be estimated. In Eq. 2, the nominal wavelength is λ_D, the design focal length is f_D, and the nominal index of refraction is n_D. By using Eq. 2 it demonstrates how the different wavelengths will slightly alter the focal distance of the laser beam through the lens. Knowing that the lenses used before the focal point in the FLDI are all the same N-BK7 Glass, it can be estimated which wavelength will focus first from Eq. 2. Using the glass's known properties Fig. 1 shows that the 532 nm, or green light, is estimated to focus at a shorter distance than the red light.

III. Experiment Setup

A. Chromatic FLDI

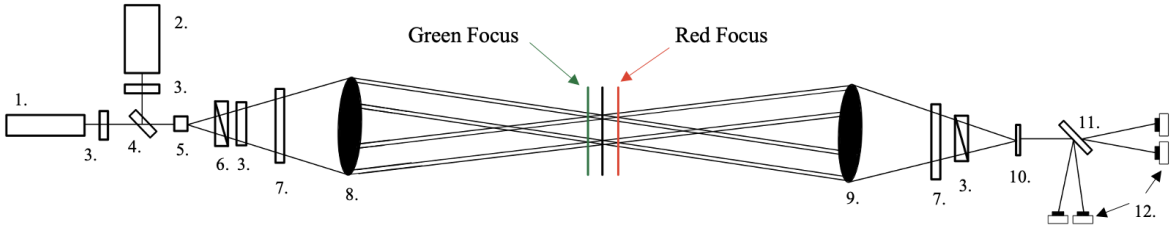

1. **He-Ne laser**
2. **Green Diode laser**
3. **Polarizer**
4. **Dichroic Mirror (Red Long-pass)**
5. **Plano-Concave Lens (- 9 mm)**
6. **1.5° Wollaston Prism**
7. **1.5-Arcminute Wollaston Prism**
8. **Plano-Convex Lens (200 mm)**
9. **Achromatic PCX Lens (200 mm)**
10. **PCV Lens (-30 mm)**
11. **Dichroic Mirror (Green Short-pass)**
12. **Photodetector**

Fig. 2 This drawing of the FLDI system is setup and symmetrical around the average the two focal locations of the green and red light. All of the optics used within the experiment are labeled in this schematic and this figure is not to scale.

Figure 2 demonstrates the experimental optical set up of the FLDI with two lasers. A red HeNe laser (lumentum 1135P) 632 nm was passed through a polarizer (Thorlabs LPVISE200-A) and was set to 45-degree polarization. Then, a green diode laser of 532nm (Edmund Optics #35-072) was set to 45-degree polarization through a polarizer (Thorlabs LPVISE200-A), and a dichroic mirror (Thorlabs DMLP605L) was used to turn the 532 nm light and allow the 632 nm light to pass through; thus, the two lasers are colinear. Once the two lasers were aligned on the same optical path, the beams were expanded through a f =-9 mm plano-concave (PCV) lens. The two beams were split into orthogonally polarized beams with a 1.5-degree Wollaston prism (United Crystal).

An additional polarizer and Wollaston prism are important to achieve two beam pairs in the FLDI. Therefore, each beam is polarized again to 45-degree polarization and then split into orthogonally polarized beams with a 1.5 arcminute Wollaston prism (United Crystal). To make this an FLDI system, the beams are then focused by a f =200 mm plano-convex (PCX) lens, and the system is symmetric around the focal point. This is why the collection side begins with an achromatic f =200 mm PCX lens. The achromatic lens helps the location of the 1.5 arcminute Wollaston prism (United Crystal). There is an ideal location for the 1.5 arcminute Wollaston prism for each wavelength, and the system can only have one location of the prism. Therefore, the location of this prism will be less than ideal. However, when placed to maximize the infinity fringe for each wavelength, it only showed minor effects on the sensitivity region. To continue the symmetry, there was a 1.5-arcminute Wollaston prism (United Crystal) and a polarizer (Thorlabs LPVISE200-A). To focus the beams on the photodetectors (Thorlabs PDA36A2), a f =-30 mm PCV lens was added after the polarizer.

To differentiate the two different lasers in the data collection, a dichroic mirror (Thorlabs DMSP605L) was used to turn the 632 nm light and allow the 532 nm light to pass through, as shown in the Fig. 2, thus allowing for four photodetectors to collect data on each of the four beam pairs. All four photodetectors were hooked up to an oscilloscope (Lecroy Waverunner 1 GHz) with four channels. Channel one and two were the red laser and channels four and three were the green laser.

The final f =-30 mm PCV lens was fused silica, but all other lenses used in this system were N-BK7 glass. The final system had 4 beam pairs along both the x-axis and z-axis, thus data collected in three dimensions.

B. Turbulent Jet

Fig. 3 demonstrates the experimental setup of the turbulent jet experiment. To test the sensitivity of the chromatic FLDI setup, a simple nitrogen tube jet (exit diameter of 4 mm) was injected orthogonally to the beam path. The dry nitrogen was in a compressed gas cylinder at 40 psi. To achieve a fully developed turbulent flow, the jet was placed 8 cm away from the FLDI focal points and slowly translated along the optical axis in a way that the flow was in the same plane as the FLDI point distribution. [17]

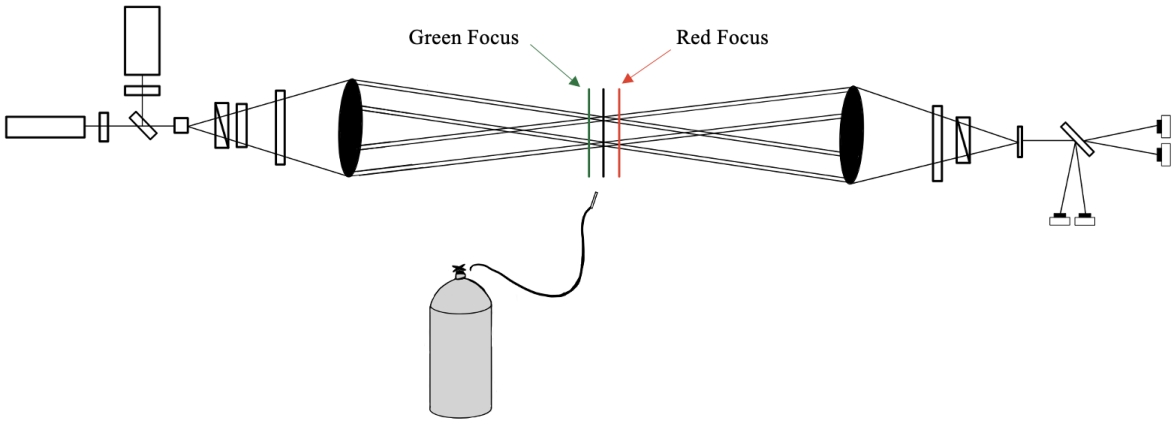

Fig. 3 Schematic showing the arrangement of optics for the additional turbulent jet. This figure is not to scale.

IV. Results

A. Focal Planes

Initially, the focal lengths for each wavelength used in this experiment were determined. To accomplish this, a matrix-based ray trace code, originally only for multi-point FLDI systems, was adapted to accommodate the additional laser included in this experimental setup. The adaptations were in accordance with Eq. 2. Within this computational method for solving for the focal lengths, only the lenses underwent the adaptation. Also, all of the lenses before the focal region were N-BK7 glass [15] and the index of refraction is shown in Fig. 1. Through the use of Fig. 1 and the computational method it was determined that the green light should focus before the red light. Within the experiment it was determined that the green light did focus before the red light with a separation of 8.6 mm along the optical axis. The ray trace shows four beam pairs because of the two Wollaston prisms within the experiment. Figure 4 shows the solution from the matrix-based ray trace code. In this figure, it visually represents how the green light will focus before the red light.

Within the actual experiment, a beam profiler (Newport LBP2) was placed colinear to the optical path. Then, it was incrementally moved along the beam path from the first to the second plano-convex lens. At each location the shutter was manual turned off for the red laser as an image was take of the green laser. This was repeated for the image of the green laser and finally an image was taken with both laser's shutters open. Figure 5 represents the processed images taken by the beam profiler. The images show how the calculations were correct and the green did in fact, focus before the red light. Table 1 shows the spacing between each beam; this was determined through the measurements of the focal

point along the optical axis. Through the calculations and the experiment it proves that the green light focused before the red light on the optical axis of the FLDI, the separation between each focal point is about 8.6 mm.

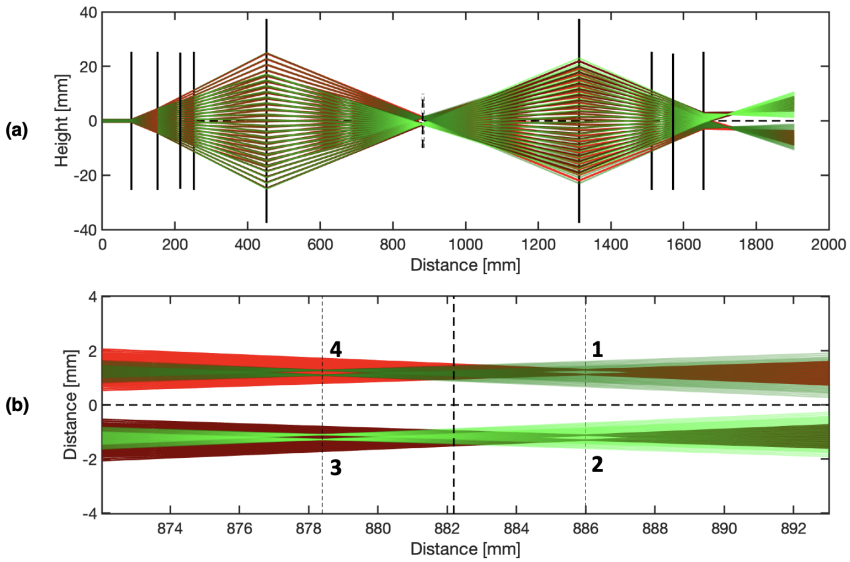

Fig. 4 Equation 2 was used to develop this code to estimate which wavlength will focus first (a) The ray trace of the entire FLDI setup. (b) The focal region of both wavelengths.

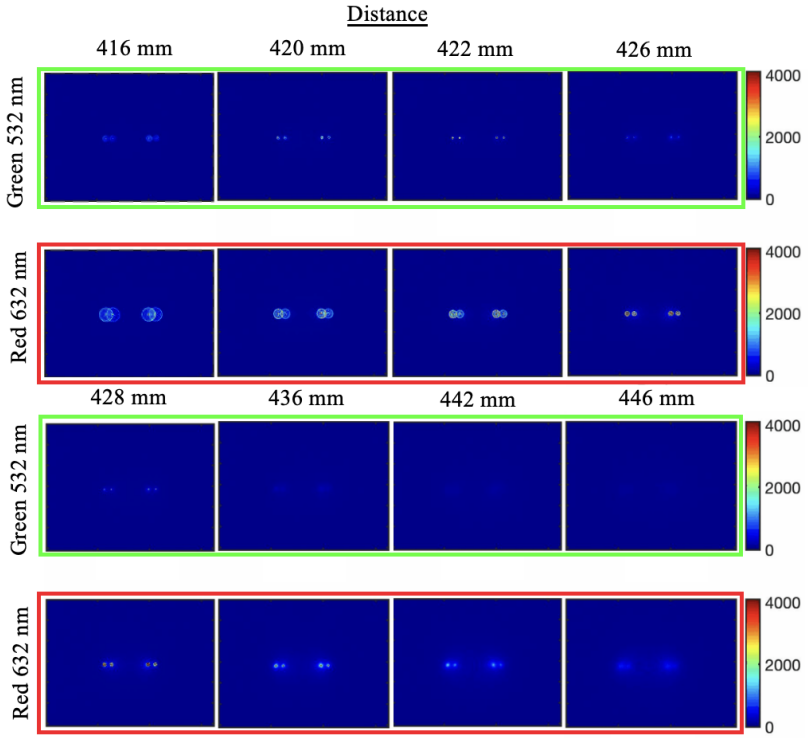

Fig. 5 These images are taken by the beam profiler and represent the red and green light focusing along the optical path. The image shows how the green focuses before the red light.

Table 1 Summary of FLDI spacing measurements at focus.

Measurement	532 nm Beam	632 nm Beam
Inner Pair Spacing [µm]	305	310
Spacing Between Pairs [mm]	1.883	1.892
$1/e^2$ Beam Radius [µm]	26	134

B. Turbulent Jet Measurements

The turbulent jet experiment was done to determine if the sensitivity region was still working as intended for an FLDI system. Other than the two focal points, there should be minimized path integration of signals, and the highest response should be at the focal region. Figure 6 shows the frequency spectra at the focal region of the FLDI system, which is approximately 43.5 cm from the first focusing lens. This frequency spectra shows the energy cascade from the large eddies to the small eddies, the Kolmogorov energy cascade, demonstrating the full turbulent spectrum. Each of the turbulent frequency responses is 100 kHz and the background peak frequency is about 300 kHz. These results show that the highest response from the system is in fact the focal region of the four beam pairs.

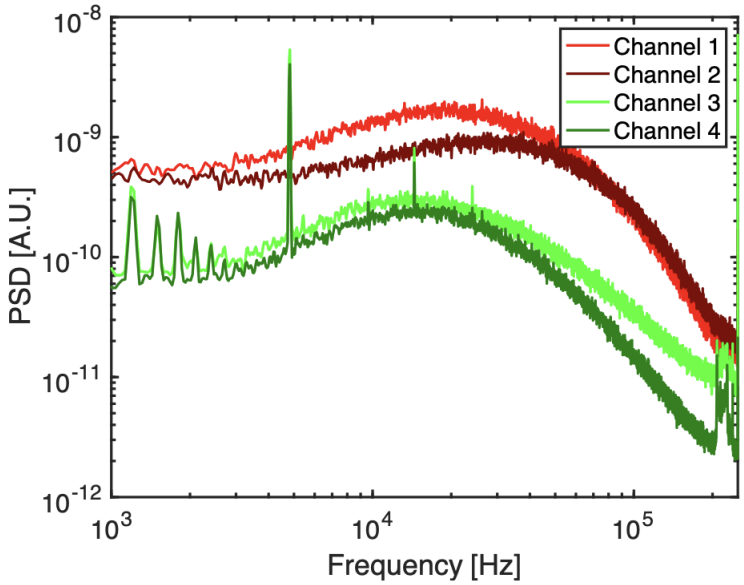

Fig. 6 The spectra at about 43.5 mm, or focal region, from the first plano-convex lens. This turbulence spectra shows the energy cascade of the from the large turbulent eddies to the smaller ones.

Table 2 Summary of Velocity Measurements.

Beam Pair	Velocity	Correlation Coefficient
Red	135.4 m/s	0.4
Green	134.4 m/s	0.23

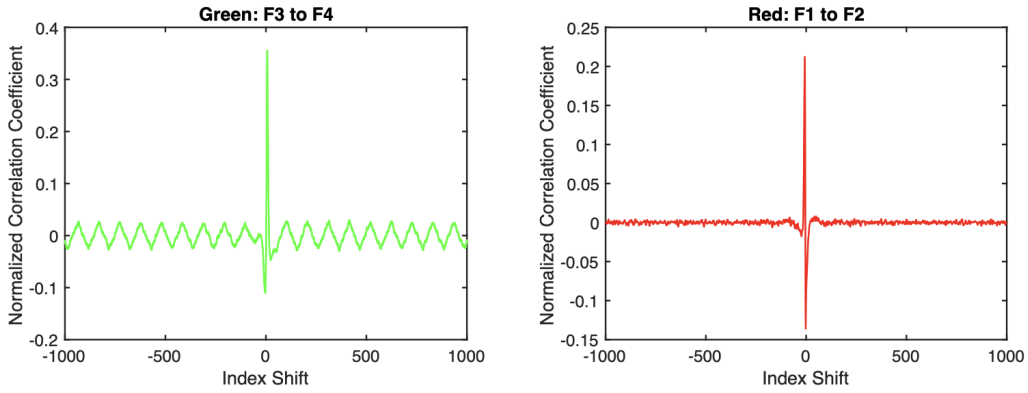

Fig. 7 These represent the normalized correlation coefficient for the correlation between the two green beam pairs and the two red beam pairs.

It is important to recognize that these correlation coefficients could be stronger but the two velocity readings are very close to each other. This proves that each wavelength can measure and calculate the same speed. The green beam pairs measured a velocity of 134.4 m/s and the red beam pairs measured a velocity of 135.4 m/s. When continuing this research it would be necessary to use a more uniform flow disturbance like a laser induced blast wave. This would also have a know speed, the speed of sound, which would eliminate the unknown velocity of the flow of the turbulent jet experiment [18, 19]. Figure 7 shows the correlation coefficient for the correlation between the two red beams and the correlation between the two green beams. These values are 0.4 and 0.23 respectively, found in table 2. This new advancement to the FLDI system was able to sucessfully measure velocity readings on both the x and z planes.

V. Summary and Conclusions

In summary, this paper reviewed a current advancement in the focused laser differential interferometry system. The system has two lasers with different wavelengths to create multiple beam pairs along the optical axis on different planes to measure three-dimensional flow. By ray trace calculations, the focal locations of the beam pairs were estimated and proved with the beam profiler. Then with the simple turbulent jet experiment, the sensitivity regions showed its ability to still minimize the path integrated signals. Both beam pairs were still able to use cross-correlation to calculate the velocity readings of the flow disturbance at the focal region. The next step would be to add an experiment with a known velocity like a laser induced blast wave, the speed of sound. Then the green and red beam pairs can be cross correlated to receive velocity readings, therefore three-dimensional flow. In this experiment, four photo detectors were used to capture the data from the FLDI. Using two RGB color photo detectors or a color camera would be better for the data collection [10, 20–22]. It would be possible to include a diffractor so the beam pairs would create a three-dimensional rectangular prism. Another option would be to use an SLM to shape the beam pairs to any configuration to fit the shape of the model in the experiment [14]. This would allow the beam pairs to resolve more boundary layer transition data along the whole shape of any said model. To continue this research, testing more wavelengths with a larger and shorter separation distance at the focal region would be important to determine the limits of this new FLDI system.

Acknowledgments

The authors would like to acknowledge Kirk Davenport and Nicholas Webber of UTSI for useful discussions during the setup.

Disclosures

The authors declare no conflicts of interest.

Data Availability Statement

Data for this work is available per reasonable request to the authors.

References

[1] Davenport, K., and Gragston, M., "Simultaneous Velocity Profile and Scalar Spectra with Linear Array-Focused Laser Differential Interferometry," *AIAA Journal*, Vol. 61, No. 2, 2023, pp. 934–939.

[2] Ceruzzi, A., Callis, B., Weber, D., and Cadou, C. P., "Application of focused laser differential interferometry (FLDI) in a supersonic boundary layer," *Aiaa scitech 2020 forum*, 2020, p. 1973.

[3] Schmidt, B. E., and Shepherd, J., "Analysis of focused laser differential interferometry," *Applied optics*, Vol. 54, No. 28, 2015, pp. 8459–8472.

[4] Lawson, J. M., *Focused laser differential interferometry*, California Institute of Technology, 2021.

[5] Neet, M. C., Lawson, J. M., and Austin, J. M., "Design, alignment, and calibration of a focused laser differential interferometer," *Applied Optics*, Vol. 60, No. 26, 2021, pp. 7903–7909.

[6] Smeets, G., and George, A., "Gas-dynamic investigations in a shock tube using a highly sensitive interferometer," *Translation of ISL Internal Report 14*, Vol. 71, 1971.

[7] Jewell, J. S., Hameed, A., Parziale, N. J., and Gogineni, S. P., "Disturbance speed measurements in a circular jet via double focused laser differential interferometry," *Aiaa scitech 2019 forum*, 2019, p. 2293.

[8] Houpt, A., and Leonov, S., "Cylindrical focused laser differential interferometer," *AIAA Journal*, Vol. 59, No. 4, 2021, pp. 1142–1150.

[9] Hopkins, K. J., Porat, H., McIntyre, T. J., Wheatley, V., and Veeraragavan, A., "Measurements and analysis of hypersonic tripped boundary layer turbulence," *Experiments in Fluids*, Vol. 62, 2021, pp. 1–12.

[10] Gragston, M., Price, T., Davenport, K., Zhang, Z., and Schmisseur, J. D., "Linear array focused-laser differential interferometry for single-shot multi-point flow disturbance measurements," *Optics Letters*, Vol. 46, No. 1, 2021, pp. 154–157.

[11] Gragston, M., Price, T. J., Davenport, K., Schmisseur, J. D., and Zhang, Z., "An m by n FLDI array for single-shot multipoint disturbance measurements in high-speed flows," *AIAA Scitech 2021 Forum*, 2021, p. 0599.

[12] Gladstone, J. H., and Dale, T. P., "XIV. Researches on the refraction, dispersion, and sensitiveness of liquids," *Philosophical Transactions of the Royal Society of London*, , No. 153, 1863, pp. 317–343.

[13] Settles, G. S., *Schlieren and shadowgraph techniques: visualizing phenomena in transparent media*, Springer Science & Business Media, 2001.

[14] Holladay, S., and Zhang, Z., "Programmable focused laser differential interferometer with a spatial light modulator as a dynamic diffractive optical element," *Opt. Lett.*, Vol. 48, No. 19, 2023, pp. 5001–5004.

[15] SCHOTT-Corporation, "Schott Optical Glass Data: Schott N-BK7," , .

[16] Hecht, E., *Optics*, Pearson Education, 2012.

[17] Pope, S. B., *Turbulent flows*, Cambridge university press, 2000.

[18] Lester, L., and Gragston, M., "10 kHz laser-induced schliere anemometry for velocity, Mach number, and static temperature measurements in supersonic flows," *Applied Optics*, Vol. 60, No. 28, 2021, pp. 8644–8650.

[19] Chism, J. R., Gragston, M., Hagen, B., Leicht, J., and Riley, Z. B., "Laser-induced schliere anemometry in a Mach 6 flow with collinear light entry," *Applied Optics*, Vol. 61, No. 11, 2022, pp. 3070–3076.

[20] Chism, J. R., Gragston, M., Peltier, S. J., and McManus, T. A., "Measurements of a Mach 2.3 turbulent boundary layer using high-speed imaging of linear array-FLDI," *AIAA Aviation 2022 Forum*, 2022, p. 3474.

[21] Benitez, E. K., Leger, T. J., Tufts, M. W., Borg, M. P., and Hill, J. L., "Hypersonic Transitional Boundary-Layer Profile using a Linear-Array FLDI," *AIAA AVIATION 2023 Forum*, 2023, p. 4253.

[22] "Linear and 2D arrays for Focused Laser Differential Interferometry using a high-speed camera," *Optics Communications*, Vol. 546, 2023, p. 129754.